

MAGIC Electromagnetic FDTD-PIC Code Dense Plasma Model Comparison with LSP

Andrew J. Woods* and Lars D. Ludeking

Alliant Techsystems (ATK), 8560 Cinderbed Road, Suite 700, Newington, VA 22122, USA

Abstract: The MAGIC *electromagnetic (EM) finite difference-time domain (FDTD) particle-in-cell (PIC)* code with a hybrid particle-fluid plasma model is compared to the LSP code by applying both to common dense plasma air ionization test problems. Agreement of maximum responses within one percent is demonstrated.

Keywords: MAGIC, EM FDTD PIC code, dense plasma, hybrid fluid, pinched electron beam, LSP.

BACKGROUND

The MAGIC electromagnetic (EM) finite difference-time domain (FDTD) particle-in-cell (PIC) code [1] contains an air ionization, hybrid particle-fluid dense plasma physics model, similar to that in the LSP (Large Scale Plasma) code [2]. LSP has been applied to a number of EM plasma investigations in recent years [3-5]. MAGIC users also model gas plasmas. Comparison of results using the MAGIC model with the more recent (2005) LSP model results is considered prudent and instructive.

INTRODUCTION

MAGIC FDTD PIC code [1] EM responses using the hybrid particle-fluid dense plasma model are compared with LSP [2] in this work. Excellent agreement between the tools is achieved when using simple geometric representations of generic electron beam chamber experiments. Validation of the models, in toto, is demonstrated. The desired goal of this comparison is the demonstration of agreement of key responses within approximately one-percent (1%). The essential physics equivalence of the respective plasma models is, of course, required to meet this objective.

The approach taken is to first compare computations on a simple, small, empty, square duct; and then proceed to a more complex system, representative of a large area electron beam experiment. These configurations facilitate highly resolved investigations of the plasma cell behavior. Both problem configurations are first run for the vacuum condition to ensure code agreement in the simplest phenomenological case. The square duct configuration focuses on the electric field, which is the primary driver of the plasma fluid model. The pinched beam stresses the codes over a wide range of phenomena including zone-by-zone air plasma breakdown and transition from electric to magnetic field determination of relativistic electron trajectories.

This paper presents models as found in the codes, and references their development. Important algorithm parameter settings necessary for proper finite difference fidelity to the

models are identified. Proper numerics are necessary for agreement between the codes which may differ in some implementation details.

MAGIC AND LSP CODES

The MAGIC Tool Suite and the LSP Suite are proprietary engineering and scientific computational physics software suites which employ the FDTD-PIC methodology. Both of these software packages are currently available as licensed commercial software products to the international research community. These FDTD-PIC applications provide the capability to model and simulate a wide variety of vacuum electronics problems and beam-wave interaction issues. Both contain specialized packages of algorithms to address broad sets of problems and research issues. Both suites are available for execution on Windows operating system (OS) and Linux/Unix OS platforms. The MAGIC Tool Suite is designed principally for use on Windows OS systems, and emphasizes vacuum electronics applications and moderate beam and plasma density interactions. Although the LSP suite is primarily designed for use in a Unix/Linux environment, it can be used in a Windows OS environment as well. It has been used primarily for dense plasma and intense beam wave interactions. Both packages include eigenmode solvers as well as dynamic time domain algorithms.

The MAGIC Tool Suite is a user-configurable electro-magnetic particle-in-cell simulation code used for the modeling and simulation of beam wave interactions and particularly for electro-energetic modeling of processes that involve interactions between space charge and electro-magnetic fields. MAGIC simulations begin from a specified initial state, usually vacuum with zero fields and no particles, although arbitrary fields and particles can be specified. MAGIC then simulates physical processes as they evolve in time. It makes use of Maxwell's time-dependent equations (specifically Faraday's law and Ampere's law) to obtain the time dependent electromagnetic fields. In addition, in the presence of particles, it solves the complete Lorentz force equation to obtain relativistic particle trajectories. The continuity equation is solved to provide current and charge densities for Maxwell's equations. This approach provides

*Address correspondence to this author at the Alliant Techsystems (ATK), 8560 Cinderbed Road, Suite 700, Newington, VA 22122, USA; Tel: (703)-254-2416; Fax: (703)-339-6953; E-mail: Andrew.Woods@atk.com

self consistent interaction between charged particles and electromagnetic fields.

MAGIC is a general purpose FDTD-PIC engine which is user configurable. It has been provided with algorithms to represent/generate structural geometries, material properties, incoming and outgoing waves, particle emission processes, electron and ion motion, air ionization, and other phenomena.

MAGIC and LSP codes have been used in the research, design, and improvement of technologies that include microwave amplifiers, antennas, sensors, fiber optics, accelerator component design, beam propagation in vacuum & atmospheric gases, lasers, pulsed power sources, plasma switches, RF induced plasma heating, field emitter arrays, semiconductor devices, radiation reflection chambers, wave scattering, coupling analyses, bio-electric effects, radar cross section, and high power sources.

AIR PLASMA MODEL

Air ionization is caused by the impact of primary and secondary emission electrons. Primaries are energetic electron beam particles and secondaries are low energy ionization products which are also capable of ionizing neutrals. Processes of electron attachment to neutral species, recombination with ions, and neutralization of ions have been compared, but these results are not included here. The LSP generic air plasma model [6] is employed with the excluded rates set to zero.

The highly-collisional plasma resulting from the ionizations is treated as a conductivity term in Maxwell's equations. This assumes quasi-neutrality. Ions are taken to be stationary over the brief time frame covered here.

Air ionization model formulae were examined and the most up to date chosen in order to ensure consistency of the models for these detailed code comparisons. SI (MKS) units are used in the MAGIC code and in this paper (with a few standard exceptions): pressure P is in atmospheres and electron energy E_e and energy equivalent temperature T_e , in electron-volts (eV). $N=2.6868 \times 10^{25} P$ is the gas molecule number density ($\#/m^3$) using Loschmidt's number at STP. The plasma model is driven by E/P , where E is the electric field only (inductive terms ignored as unimportant).

The semi-empirical formulas presented below are combinations of analytical expressions and curve fit parameters as found in the codes. Their development is described in [6] along with test results. The expressions are presented here for documentation of the actual code inputs employed for this comparison. In general, users of MAGIC and LSP provide their own gas model representative parameter inputs when details of the media are significant.

The primary electron neutral ionization cross section is derived from the electron stopping power dE/dx of the medium:

$$\sigma_{ion} = A_0 dE/dx / (N W_{gas} c).$$

The stopping power is [6]:

$$dE/dx = A_1 N Z_{gas} Z_{eff} [\ln(A_2 I_{sq} E_e \gamma^2 \beta^2) + 1 - \beta^2] / \beta^2,$$

where: W_{gas} is the energy needed per created pair (34.0 eV); γ is the relativistic factor; β the ratio of the electron velocity to c (the vacuum speed of light); Z_{gas} is the number of bound electrons per molecule (14 used here); and $Z_{eff} = 1$. $I_{sq} = (I_{av})^{-2}$ where: $I_{av} = 80 \text{ eV}/m_e c^2$ is the average electron ionization potential ($m_e c^2 = 5.11 \times 10^5 \text{ eV}$). The empirical curve fit constants:

$$A_0 = 1.54 \times 10^{10}; A_1 = 4.98 \times 10^{-25}; \text{ and } A_2 = 0.35355;$$

are material-dependent. The expression dE/dx has an embedded factor of $m_e c^2$.

The resultant formula for σ_{ion} conservatively replicates National Institute of Standards and Technology data for dry air over the energy range utilized here.

The avalanche coefficient is:

$$\alpha(E/P) = 100c f_{ion} c_1 (E/P)^6 / (1 + c_2 E/P + c_3 (E/P)^4 + c_4 (E/P)^6) / (1.0 + T_e) / (4.0 * W_{ion})$$

where E is the electric field. Constant values of the curve fit parameters are:

$$c_1 = 7.84 \times 10^4; c_2 = 26.67; c_3 = 2242; c_4 = 691.6;$$

and $f_{ion} \sim 1.0$ is the un-ionized molecule fraction.

The electron mobility is $\mu_e (m^2/V\text{-s})$:

$$\mu_e(|E|, P, n_e) = e / (100 m_e \nu_e), \text{ where}$$

$$\nu_e = \nu_{en}(|E|, P) + \nu_{ei}(|E|, n_e).$$

The terms ν_{en} and ν_{ei} are the electron collision rates with neutrals and ions, respectively. The argument n_e is the secondary electron number density ($\#/m^3$) which is computed with the standard rate equation [1].

$$\nu_{en}(|E|, P) = 64.0 P (T_e)^{1/2} \text{ for } T_e \geq 4.0$$

$$\nu_{en}(|E|, P) = P (4.98733 + T_e (82.3167 +$$

$$T_e (-20.7957 + 1.97517 T_e)) \text{ for } T_e < 4.0$$

$$\nu_{ei}(|E|, n_e) = 4.86 \times 10^{-17} f_e (10^{-6} n_e) (T_e)^{-1.5} \ln(1.0 + 2.39 \times 10^{20} (T_e)^3 / (10^{-6} n_e))$$

where $f_e = \text{MAX}(1, 0.5 n_e / N)$ is the fractional ionization and the factor of 1/2 is for diatomic molecules.

Using $\phi = \sqrt{10^{-5} E/P / 511.0}$, the electron temperature from a least squares fit to a cubic spline is:

$$T_e = a_1 (1 + a_2 \phi (1 + a_3 \phi (1 + a_4 \phi (1 - a_5 \phi (1 - a_6 \phi (1 - a_7 \phi (1 - a_8 \phi))))))))$$

for $\phi < 0.716$ and

$$T_e = b_1 (1 + b_2 \phi) \text{ for } \phi \geq 0.716$$

where constant values are

$$a_1 = 0.155; a_2 = 8.6277; a_3 = 14.944; a_4 = 18.948;$$

$$a_5 = 5.6968; a_6 = 2.1216; a_7 = 0.92303;$$

$$a_8 = 0.33829; b_1 = 0.505; b_2 = 35.4.$$

Primary electron drag was ignored in both codes. The electron range of 3.8 m is significantly longer than the simple geometry employed here, but is comparable to the pinch geometry case.

SIMPLE GEOMETRY ELECTRON BEAM TEST

The small scale test problem is a square duct of infinite length with air at 1 atmosphere (Fig. 1). The interior cross section is 11 cm by 11 cm. The system is modeled in Cartesian coordinates with 0.5 cm zones. Electrons are emitted uniformly from the raised cathode at $y = -4.5$ cm with 1- MeV energy. The emission current density rises to 10 A/cm² in 0.25 ns and then remains constant. The results of this simple case support the more complex pinched electron beam test.

Agreement of the responses is obtained when compatible algorithm settings are used so the codes are solving the same fundamental problem description. The codes are both run in standard momentum-conserving explicit mode. LSP macroparticle positions are updated with the ‘standard’ particle kinematics option which uses the familiar Boris leapfrog scheme with the magnetic field rotation splitting the electric field push into two separate halves. Particle forces due to fields are averaged from the surrounding grid node positions in both codes. Particle conversion to current densities on the spatial grid utilizes ‘extended particles’ in LSP which stretch over two zones in the longitudinal as well as transverse velocity directions; as is done in MAGIC. MAGIC is run with the ‘centered’ Maxwell equation update corresponding to the LSP ‘explicit’. The ‘kinetic ionization’ option is used in MAGIC which, as in LSP, sums the primary ionization charge for every particle every time step (as opposed to the faster current density source ionization option). Kinetic ionization requires random emission for comparable resultant code particle trajectories for the nominal numerical grids employed here.

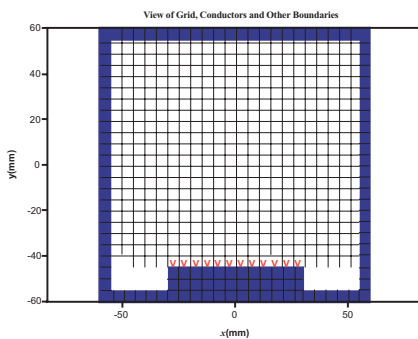


Fig. (1). Side view of duct test problem geometry for validating plasma response.

The results for the electric field at the midpoint of the second zone above the center of the cathode are shown in Fig. (2). Excellent agreement is seen for this primary driver of the air fluid models with strong quenching of the electric fields by the plasma (compared with the vacuum case). Attention can be directed with confidence to the more complex model of interest.

PINCHED ELECTRON BEAM TEST

The pinched electron beam test geometry is a cylindrical cavity containing air at 1 atmosphere (Fig. 3). The computer drawing shows the cross section in the $r z$ plane which is rotated about the symmetry axis in the codes to form the 1.2 m diameter by 4.5 m length conducting chamber. A port is used at the top right to represent the impedance of the

cathode assembly relative to the chamber. 1- MeV electrons are emitted uniformly from the end of the circular cathode over an annulus of interior radius, 15 cm and exterior radius, 30 cm. The current density rises to 3 A/cm² in 10 ns, then remains constant. The initial magnetic field is zero.

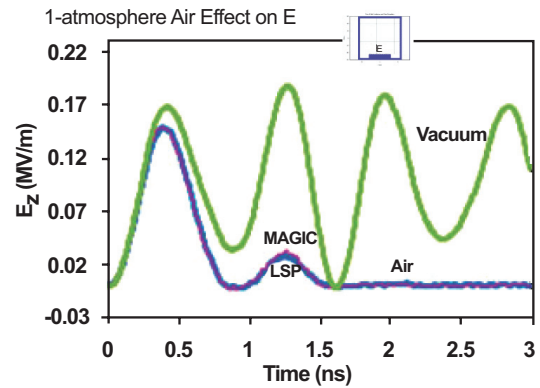


Fig. (2). Peak electric field driver of plasma model in 2D duct.

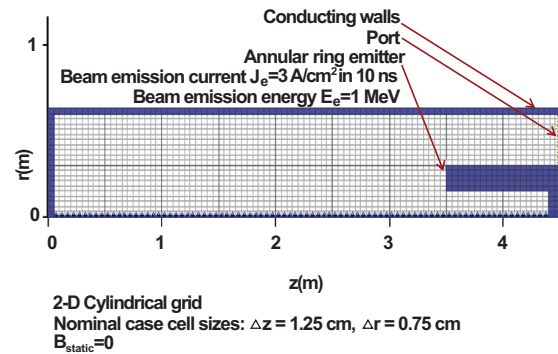


Fig. (3). Test problem geometry for pinched beam comparison.

In Fig. (4), the electron positions are shown at time 25 ns for the nominal case, and at 14 ns for 4x reduced zone sizes in Fig. (5). The modest differences in the initial pinch location decrease substantially with decreased spatial cell size (by a factor of 3 to 4). The magnetic field contours at 30 ns are shown in Fig. (6). Substantial agreement of both the positions and resulting fields are seen demonstrating that the models are converging and solving the same problem. Both codes give a maximum pinched magnetic field of ~0.018 tesla, 1.8 meters from the cathode at 30 ns.

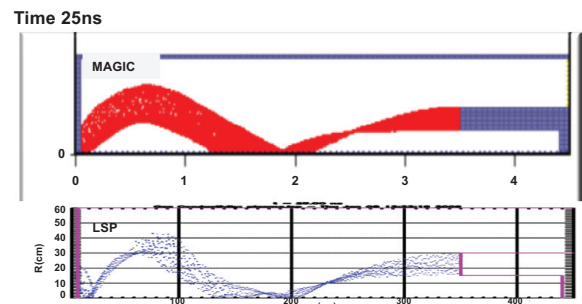


Fig. (4). Particles vs radial (vertical) and axial position at time 25 ns from MAGIC (top) and LSP for the nominal case.

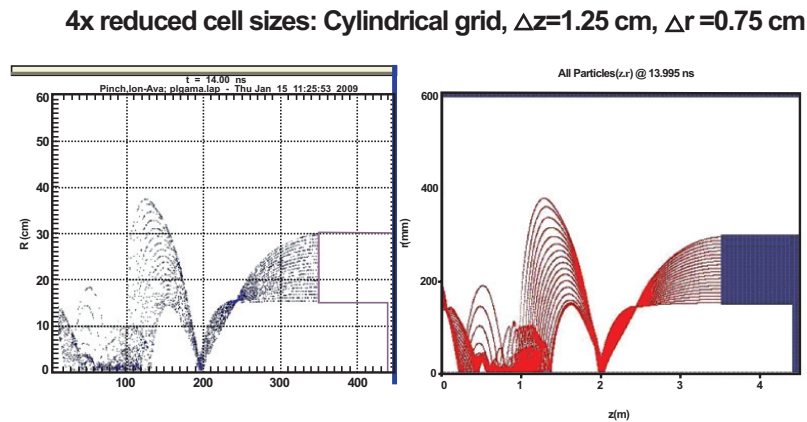


Fig. (5). Particles vs radial (vertical) and axial position at time 14 ns from MAGIC (right) and LSP for 4x decreased cell sizes ($\Delta z = 1.25$ cm, $\Delta r = 0.75$ cm).

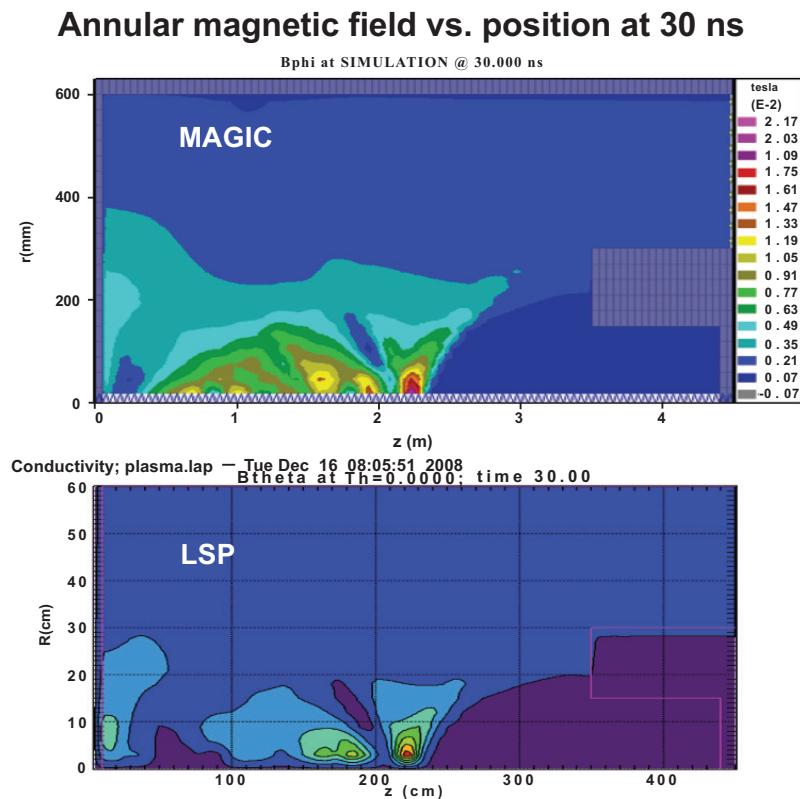


Fig. (6). Annular magnetic field vs radial (vertical) and axial position at time 30 ns from MAGIC (top) and LSP. (1 gauss = 10^4 tesla).

SUMMARY AND CONCLUSIONS

The MAGIC EM FDTD PIC code has been compared with the LSP code on air ionization test problems using simple geometric representations of generic electron beam chamber experiments. Nominally, a one-percent agreement among important maximum responses has been obtained. The pinched beam response demonstrates significant agreement of the FDTD PIC dense plasma models in toto. The zone-by-zone travelling nature of the air plasma breakdown of the electric fields causes the transition from electric to magnetic

field determination of electron trajectories thus stressing every core aspect of the codes.

Careful selection of the algorithm settings is required due largely to the size of the finite difference grids employed combined with some modest variations in the details of the code parameter settings. Statistical variations in the results are evident, but the impact of these can be made inconsequential with randomized emission, decreased time step, and increased particle numbers.

Based on results of detailed comparisons, such as the examples presented here, MAGIC code users can be

confident they will obtain responses in close agreement with LSP code analysis for dense plasmas. Upgraded air model rates, consistent with National Institutes of Standards and Technology (NIST) data, have been programmed into MAGIC versions 2.1.6 and greater. Additionally, MAGIC provides input of arbitrary gas chemistry functions by the user employing the MAGIC Control Language MCL. This enables the convenient and accurate representation of more complex gas mixtures producing dense plasmas.

The air plasma model described here for MAGIC2D has also been implemented in MAGIC3D. Additionally, the 3D code has been compared successfully with LSP 3D in much the same manner as reported in this paper [7].

ACKNOWLEDGEMENTS

This work expands on research originally sponsored by the Air Force Office of Scientific Research under contract No. FA9550-60-C-0148. The authors gratefully acknowledge the assistance of Bob Clark of Voss Scientific in understanding the workings of the LSP code.

REFERENCES

- [1] Goplen B, Ludeking L, Smithe D, Warren G. User-configurable MAGIC for electromagnetic PIC calculations, in *Computer Physics Communications* 87 1995; 54-86 available from: www.mrcwdc.com
- [2] LSP (2005) is an EM PIC plasma code product of Alliant Techsystems. Available from: <http://www.mrcwdc.com/LSP/description.html>
- [3] Rose DV, Welch DR, Thoma C, Warne LK, Jorgenson R. Computational modeling of high pressure gas breakdown and streamer formation in external electric fields. In: Schamiloglu E, Peterkin F, Eds. 2007 IEEE Pulsed Power Conference Digest of Technical Papers. New Mexico 2007; pp. 1205-8.
- [4] Thoma C, Hughes TP, Welch D, Rose D, Clark R. Hybrid Simulation Algorithms for Plasma Accelerators. In: Schamiloglu E, Peterkin F, Eds. 2007 IEEE Pulsed Power Conference Digest of Technical Papers. New Mexico 2007; pp. 1449-52.
- [5] Rose DV, Welch DR, Hughes TP, Clark RE, Mostrom CB. Plasma formation, evolution, and dynamics in 100 TW vacuum-transmission-line post-hole convolutes. In: Schamiloglu E, Peterkin F, Eds. 2007 IEEE Pulsed Power Conference Digest of Technical Papers. New Mexico 2007; pp. 171-4.
- [6] Welch DR, Olson CL, Sanford TWL. Simulation of charged-particle beam transport in a gas using a hybrid particle-fluid model. *Phys Plasmas* 1994; 1; 764-73.
- [7] Woods AJ, Ludeking LD. MAGIC3D electromagnetic FDTD-PIC code dense plasma model benchmark. In: Peterkin F, Curry R. Eds. 2009 IEEE Pulsed Power Conference (PPC-2009) Conference Proceedings. Washington D.C. 2009; pp. 533-6. Available from: <http://ppc.missouri.edu/index.html>

Received: September 8, 2009

Revised: November 5, 2009

Accepted: January 26, 2010

© Woods and Ludeking; Licensee *Bentham Open*.

This is an open access article licensed under the terms of the Creative Commons Attribution Non-Commercial License (<http://creativecommons.org/licenses/by-nc/3.0/>) which permits unrestricted, non-commercial use, distribution and reproduction in any medium, provided the work is properly cited.